The Molecular Characteristics of Poly(propyleneimine) Dendrimers As Studied with Small-Angle Neutron Scattering, Viscosimetry, and Molecular Dynamics

Rolf Scherrenberg,* Betty Coussens, Paul van Vliet, Guillaume Edouard, Josephine Brackman, and Ellen de Brabander

DSM Research, P.O. Box 18, NL-6160 MD Geleen, The Netherlands

Kell Mortensen

Risø National Laboratory, DK-4000 Roskilde, Denmark

Received December 10, 1996; Revised Manuscript Received August 1, 1997[⊗]

ABSTRACT: The molecular characteristics of the first five generations of poly(propyleneimine) dendrimers with two different types of end groups have been investigated using small-angle neutron scattering (SANS), viscosimetry, and molecular dynamics simulations. The dimension of the poly(propyleneimine) dendrimers, as measured by both SANS and viscosimetry, increases linearly with the generation number and roughly as $M^{1/3}$, where M is the molar mass of the dendrimer. This relationship proves to be independent of the character of the end group and the solvent used and is indicative of a compact (space-filling) structure with a fractal dimensionality of approximately 3. The distinct maximum in the Kratky representation of the scattering data and the observed relation (i.e., $R_\eta \simeq \sqrt{(5/3)R_g}$) between the hydrodynamic radius R_η and the radius of gyration R_g are consistent with such a structure. Molecular dynamics simulations for two different solvent qualities are in good accordance with the acquired experimental results. The probability distributions of the amine end groups, based on these simulations, exhibit a substantial degree of backfolding. The corresponding radial density distributions show a constant density plateau and a monotonic decrease of the density toward the exterior of the molecule. The above results indicate that the poly(propyleneimine) dendrimers can be considered as flexible molecules with a relatively homogeneous radial density distribution. This view clearly deviates from both the dense shell and dense core models.

1. Introduction

Dendrimers are obtained by controlled, repetitive reaction sequences, yielding regularly branched macromolecules that emanate from a central core and have a defined number of end groups. Syntheses of a number of different dendrimers via both divergent and convergent routes have been reported by several laboratories.[1−6]

Following the first synthesis of dendrimers, theoretical investigations predicted molecular dimensions, limits of growth, and intramolecular configurational details of dendrimers in an attempt to provide a fundamental explanation of their observed physical behavior like, for instance, the maximum of the intrinsic viscosity as a function of the generation number.[2,7] de Gennes and Hervet[8] analytically predicted, using a self-consistent-field model, that the dendrimer emanates radially outward from the core, with all end groups on the periphery of the molecule (*i.e.*, dense shell). On the other hand, numerical calculations of Lescanec and Muthukumar[9] predicted a density maximum in the core and the distribution of end groups throughout the molecule (i.e., dense core). Monte Carlo[10,11] and molecular dynamics simulations[12] as well as a very recent self-consistent mean-field model[13] are more or less in line with the latter model, but it has still not been affirmed experimentally. Some experimental studies on different dendrimers have been reported using, e.g., size-exclusion chromatography (SEC), viscosimetry,[2,7] ^{2}H and ^{13}C NMR[14,15] and small-angle scattering,[16−18] but the overall number is limited. The lack of experimental results is most probably connected with the poor availability of well-defined dendrimers. However, recently dendrimers became more easily available due to kilogram-scale production of up to five generations of poly(propyleneimine) dendrimers.[6]

In this study, the molecular characteristics of the poly(propyleneimine) dendrimers with two different types of end groups have been investigated for different generation numbers. For this purpose, small-angle neutron scattering (SANS) and viscosimetry have been employed. Additionally, the experimental results are compared directly with independent molecular dynamics simulations.

2. Experimental Section

2.1. Materials. The poly(propyleneimine) dendrimers, having diaminobutane as the core, were synthesized by a repetitive reaction sequence of Michael additions of acrylonitrile to the primary amine end groups followed by hydrogenation of the nitrile end groups. The reactions proceed with a selectivity higher than 99%. Five generations with both amine end groups, DAB-dendr-$(NH_2)_x$, and nitrile end groups, DAB-dendr-$(CN)_x$, were obtained (x = 4, 8, 16, 32, 64). More detailed information with respect to the synthesis and material properties can be found elsewhere.[6,19]

2.2. SANS. The SANS experiments were performed at the SANS facility of the Risø National Laboratory, Roskilde, Denmark. Three different setups were selected: (1) λ = 8 Å, D = 3 m; (2) λ = 3 Å, D = 3 m; (3) λ = 3 Å, D = 1 m (λ = wavelength, D = sample-to-detector distance). At first instance, a concentration series of DAB-dendr-$(NH_2)_{64}$ in D_2O was measured using 2-mm-thick quartz cuvettes in order to

* To whom correspondence should be addressed.

[⊗] Abstract published in *Advance ACS Abstracts,* December 15, 1997.

S0024-9297(96)01818-9 CCC: $15.00
Published on Web 01/07/1998

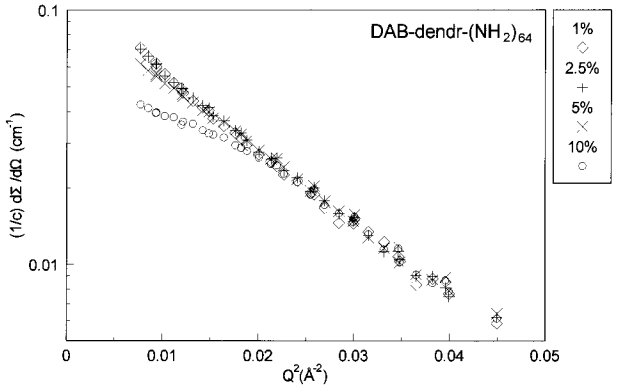

Figure 1. Guinier representation (log(dΣ/dΩ) vs Q^2) for solutions with a varying concentration of DAB-dendr-$(NH_2)_{64}$ in D_2O. For comparison, the scattered intensity has been divided by the concentration.

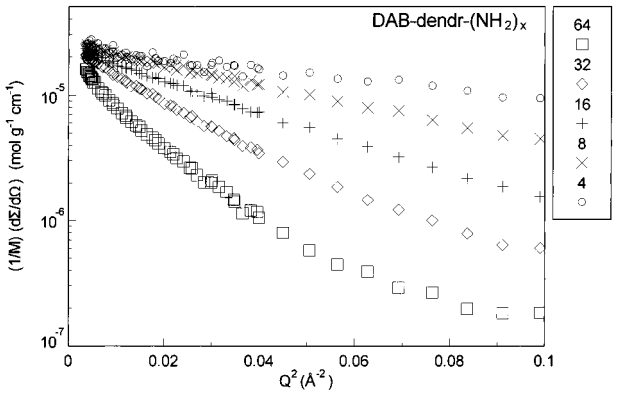

Figure 2. Guinier representation (log(dΣ/dΩ) vs Q^2) for 1% (v/v) DAB-dendr-$(NH_2)_x$ in D_2O. For comparison, the scattered intensity has been divided by the molar mass.

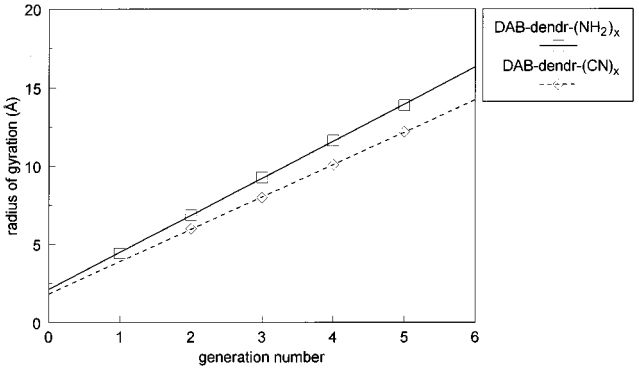

Figure 3. Radius of gyration versus the generation number for 1% (v/v) solutions of DAB-dendr-$(NH_2)_x$ and DAB-dendr-$(CN)_x$ in D_2O and acetone-d_6, respectively.

investigate concentration effects. A concentration of 1% (v/v) proved to be the optimal concentration with respect to the scattered intensity and negligible interparticle interference effects (Figure 1). The contribution of the interparticle interference $S(Q)$ becomes apparent at a concentration of about 5%(v/v).

The DAB-dendr-$(NH_2)_x$ dendrimers were measured in D_2O and methanol-d_4. The DAB-dendr-$(CN)_x$ dendrimers were studied in acetone-d_6 and THF-d_8. All deuterated solvents were purchased from Campro Scientific. No noticeable effects were observed as a result of the deuterium exchange of the amine groups in DAB-dendr-$(NH_2)_x$ with the solvent. Similar scattering data were obtained with small-angle X-ray scattering (SAXS).[20]

The radially averaged scattering patterns were corrected for absorption, solvent scattering, and instrumental background and converted into an elastic scattering cross-section using water as a secondary standard. The corrected scattering patterns, measured at the different setups, were combined using a least-squares fitting procedure of the overlapping regions. The radius of gyration R_g was calculated by applying the Guinier approximation.[21]

In contrast to DAB-dendr-$(CN)_{64}$, the SANS patterns of 1% (v/v) DAB-dendr-$(NH_2)_{64}$ in D_2O and methanol-d_4 showed some excess scattering at low Q ($Q < 0.01$ Å^{-1}), indicative of aggregation of the dendrimer molecules. This phenomenon was confirmed by independent dynamic light scattering experiments[22] and proved to be related to the presence of a small fraction of non-hydrogenated DAB-dendr-$(CN)_{64}$. Recent SANS experiments have shown that the excess scattering is absent and the radius of gyration is unaltered after removal of this fraction by extraction.[23]

2.3. Viscosimetry. The viscosity measurements were performed in an Ubbelohde viscometer at 25 °C. The intrinsic viscosity [η] was determined by extrapolation of the reduced viscosity η_{sp}/c, determined at four different concentrations, to infinite dilution. The viscosities of DAB-dendr-$(NH_2)_x$ and DAB-dendr-$(CN)_x$ were determined in D_2O (Campro Scientific) and acetone, respectively. The hydrodynamic radius R_η was calculated from the intrinsic viscosity data by applying the Einstein equation for hard spheres.[24]

2.4. Molecular Dynamics. The five generations of DAB-dendr-$(NH_2)_x$ were constructed by means of the builder facility of the BIOSYM package,[25] which was running on a Silicon Graphics Indigo computer. For the higher generations reasonable structures were obtained by combining energy minimization and high-temperature (1500 K) molecular dynamics (MD) runs. These were carried out by means of the Discover2.95 program,[25] employing the consistent valence force field (CVFF). Cross-terms were neglected and the bond stretch potential was described by means of a harmonic potential instead of the more accurate Morse function. For the calculation of the radii of gyration, two different models based on CVFF were considered, i.e., CVFFC and CVFFREP. In CVFFC both the Coulombic and the van der Waals (VDW) interactions between the nonbonded atoms were included. In CVFFREP only the repulsive VDW energy terms were taken into account. Using each of these models, the structures of DAB-dendr-$(NH_2)_x$ were first energy minimized until the maximum energy derivative was less than 0.01 kcal/mol·Å and then subjected to a molecular dynamics run at room temperature (300 K). The time step was chosen to be 1 fs, and the equilibration time was taken to be 25 ps. After equilibration every 250th configuration was stored and a total of 1000 configurations were generated.

The small-angle scattering curves as well as the probability distribution of the amine end groups were calculated using standard routines in the Discover2.95 program.[25] The average radial density distribution was calculated using an in-house developed software program.[26]

3. Results and Discussion

The SANS patterns of 1% solutions of DAB-dendr-$(NH_2)_x$ in D_2O are illustrated for different generation numbers in Figure 2, using a Guinier representation (log(dΣ/dΩ) vs Q^2). A linear dependence is observed for all generation numbers. The increase of the slope with the generation number is connected with the corresponding increase of the dendrimer dimensions. The observed nonlinear dependence for the fourth and fifth generation at high wave vectors (Figure 2) is related to the fact that in this region $QR_g > 1$ and therefore the Guinier approximation no longer holds.

The obtained radii of gyration (Figure 3 and Tables 1 and 2) show a linear relationship with the generation number. Similar results have been obtained for 1% solutions of DAB-dendr-$(CN)_x$ in acetone-d_6 (Figure 3), although the absolute dimensions are consistently

Table 1. Specific Data of the Amine-Terminated Poly(propyleneimine) Dendrimer DAB-dendr-$(NH_2)_x$

generation	sample code	molar mass (g/mol)	no. of end groups	$[\eta]^{25\ °C}$ (dL/g)	V_η (Å^3)	R_η (Å)	R_g(SANS) (Å)	R_g(CVFFC) (Å)	R_g(CVFFREP) (Å)
1	DAB-dendr-$(NH_2)_4$	317	4	0.045	948	6.1	4.4	4.9	5.0
2	DAB-dendr-$(NH_2)_8$	773	8	0.055	2824	8.8	6.9	6.0	7.6
3	DAB-dendr-$(NH_2)_{16}$	1687	16	0.062	6947	11.8	9.3	7.4	10.1
4	DAB-dendr-$(NH_2)_{32}$	3514	32	0.068	15872	15.6	11.6	10.0	12.9
5	DAB-dendr-$(NH_2)_{64}$	7168	64	0.068	32367	19.8	13.9	12.5	15.9

Table 2. Specific Data of the Nitrile-Terminated Poly(propyleneimine) Dendrimer DAB-dendr-$(CN)_x$

generation	sample code	molar mass (g/mol)	no. of end groups	$[\eta]^{25\ °C}$ (dL/g)	V_η (Å^3)	R_η (Å)	R_g(SANS) (Å)
1	DAB-dendr-$(CN)_4$	300	4	0.024	478	4.9	
2	DAB-dendr-$(CN)_8$	741	8	0.030	1477	7.1	6.0
3	DAB-dendr-$(CN)_{16}$	1622	16	0.034	3663	9.6	8.0
4	DAB-dendr-$(CN)_{32}$	3385	32	0.035	7869	12.3	10.1
5	DAB-dendr-$(CN)_{64}$	6910	64	0.036	16523	15.8	12.2

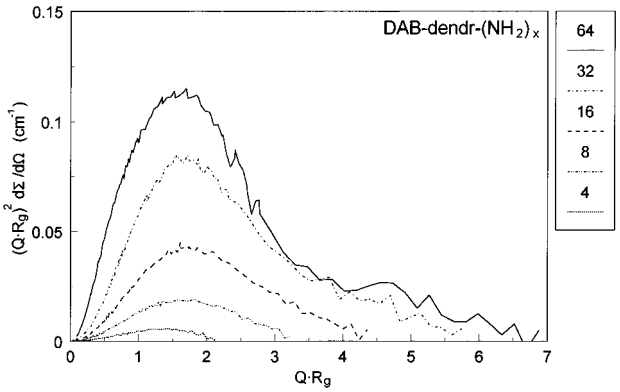

Figure 4. Modified Kratky representation for 1% (v/v) DAB-dendr-$(NH_2)_x$ in D_2O. For comparison, the dependence of the length scale has been removed by plotting $(QR_g)^2\ d\Sigma/d\Omega$ versus QR_g.

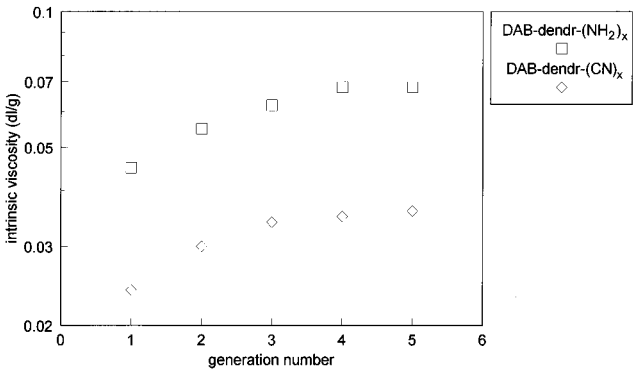

Figure 5. Intrinsic viscosity of DAB-dendr-$(NH_2)_x$ and DAB-dendr-$(CN)_x$ as a function of the generation number.

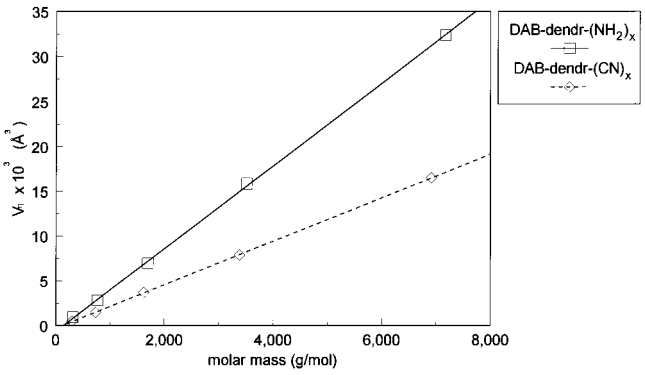

Figure 6. Hydrodynamic volume V_η versus the molar mass for DAB-dendr-$(NH_2)_x$ and DAB-dendr-$(CN)_x$.

smaller than those for DAB-dendr-$(NH_2)_x$. The obtained R_g for DAB-dendr-$(NH_2)_x$ in methanol-d_4 and DAB-dendr-$(CN)_x$ in THF-d_8 were, within experimental error, similar to those in D_2O and acetone-d_6.

The relatively larger dimensions of DAB-dendr-$(NH_2)_x$ in comparison to DAB-dendr-$(CN)_x$ must be related to the different character of the end groups (i.e. polarity) which dominates the physical properties of the dendrimer with respect to e.g. solubility, basicity and aggregation. For instance, DAB-dendr-$(NH_2)_x$ is soluble in relatively polar solvents such as water and methanol whereas DAB-dendr-$(CN)_x$ is soluble in relatively apolar solvents like acetone and THF.

A modified Kratky representation of the form factor of DAB-dendr-$(NH_2)_x$ (Figure 4) shows a distinct maximum at about $QR_g = 1.5-2$ for all generation numbers and possibly a weak secondary Kratky peak at $QR_g = 4-5$ for the fifth generation. Such a distinct maximum in the Kratky representation has also been reported for star polymers but does not appear for linear polymers.[27] The shape and the position of the maxima are in very good agreement with theoretical predicted Kratky representations.[10,13]

The variation of the intrinsic viscosity $[\eta]^{25\ °C}$ with the generation number (Figure 5) is comparable with that reported for other dendrimers,[2,7] although the absolute change of $[\eta]^{25\ °C}$ is relatively small and no maximum of the intrinsic viscosity is observed up to fifth generation.

This is not surprising regarding the fact that, up to the fifth generation, the hydrodynamic volume V_η scales almost linearly with the molar mass (Figure 6).

The hydrodynamic volume V_η and the hydrodynamic radius R_η calculated on the basis of intrinsic viscosity data are listed in Tables 1 and 2. The relatively smaller dimensions of DAB-dendr-$(CN)_x$ in comparison with DAB-dendr-$(NH_2)_x$ are in accordance with the SANS data. Noteworthy is the fact that the dimensions of the poly(propyleneimine) dendrimers are consistently smaller as compared to the poly(amidoamine) (PAMAM) dendrimers.[2] This is related to the relatively longer segment length and higher core multiplicity of the PAMAM dendrimers.

A double-logarithmic representation of R_η versus the molar mass (Figure 7) shows for both dendrimer types a reasonable linear relationship with a slope of approximately 0.37. This implies that volume and mass increase almost equally with the generation number. The exponent is close to the limiting case $R \propto M^{1/3}$ for a compact (space filling) structure.

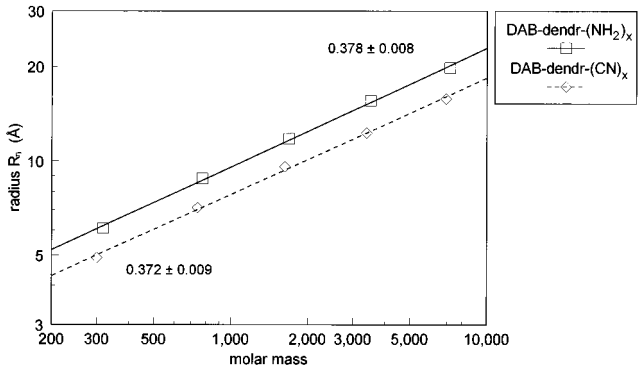

Figure 7. Double-logarithmic representation of the hydrodynamic radius versus the molar mass for DAB-dendr-$(NH_2)_x$ and DAB-dendr-$(CN)_x$.

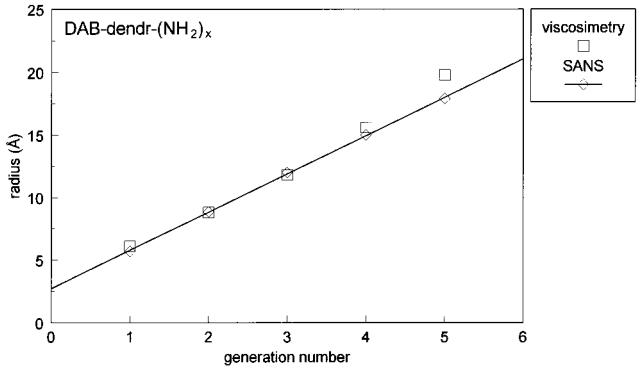

Figure 8. Comparison of the hydrodynamic radius R_η with $\sqrt{(5/3)}R_g$ for 1% solutions of DAB-dendr-$(NH_2)_x$ in D_2O.

The hydrodynamic radius of such a compact structure should be related to the radius of gyration as $R_\eta \simeq \sqrt{(5/3)}R_g$. A direct comparison between R_η and $\sqrt{(5/3)}$-R_g for DAB-dendr-$(NH_2)_x$ shows a very reasonable agreement (Figure 8). For the higher generation number the ratio between R_η and R_g becomes somewhat larger than $\sqrt{(5/3)}$ which could be indicative of a structure with a denser center.[28−30]

The observed dependence of the molecular dimension on the molar mass for the poly(propyleneimine) dendrimers is not in agreement with the self-consistent-field model of de Gennes and Hervet[8] nor with numerical calculations of Lescanec and Muthukumar.[9] The former model predicts $R \propto M^{0.2}$, which not only deviates from our findings but is also rather unlikely because it implies a consistent decrease of the intrinsic viscosity with the generation number (i.e., $[\eta] \propto M^{-0.4}$). A maximum in the intrinsic viscosity is, on the other hand, predicted by the model of Lescanec and Muthukumar,[9] but the calculated $R \propto M^{0.5}$ for small generation numbers and $R \propto M^{0.2}$ for large generations is not in agreement with our experimental results. Our results are, however, in line with the recent molecular dynamics study of Murat and Grest.[12] On the basis of molecular dynamics simulations, under varying solvent conditions, these authors predict a compact (space-filling) structure under all solvent conditions, with the radius of gyration scaling with the number of monomers N as $R_g \propto N^{1/3}$.

In order to be able to compare our experimental results directly with the theoretical investigations,[9−13] we performed a molecular dynamics study for DAB-dendr-$(NH_2)_x$ with two different force fields. The two force fields used, i.e., CVFFC and CVFFREP, represent respectively the limiting cases of bad and good solvent qualities.[31] The average conformations (Figure 9a) as obtained with the CVFFC force field (i.e., bad solvent) show more collapsed structures with some degree of backfolding, whereas the CVFFREP force field (i.e., good solvent) gives rise to more extended structures (Figure 9b).

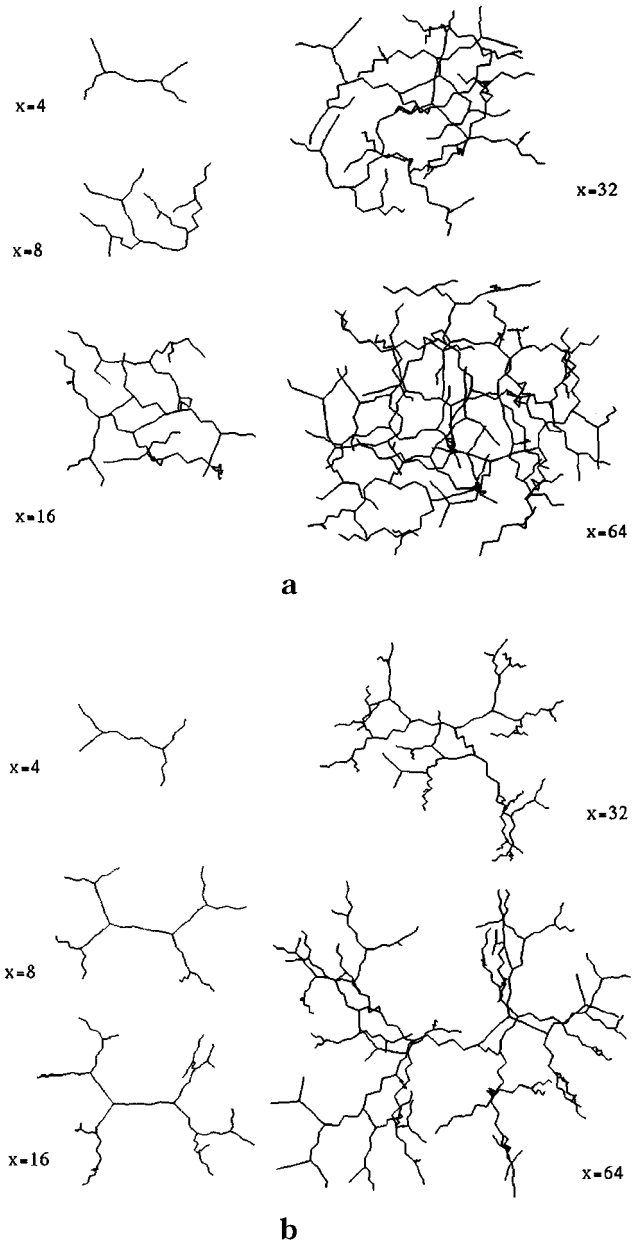

Figure 9. Average conformations as obtained from molecular dynamics simulations at room temperature for the different generations of DAB-dendr-$(NH_2)_x$ using the CVFFC (a) and CVFFREP (b) force fields.

Double-logarithmic representations of the small-angle scattering curves, calculated on the basis of the two different force fields (Figure 9), and the experimentally obtained scattering curve for a 1% (v/v) solution of DAB-dendr-$(NH_2)_{64}$ in D_2O are depicted in Figure 10. The theoretical scattering curves have been scaled to the experimental scattering curve in the low-Q region. In contrast to the scattering curve obtained for the CVFFC force field, the scattering curve for the CVFFREP force field shows intensity maxima which are characteristic of a spherical structure. The experimental scattering intensity curve, which lies nicely in between the two

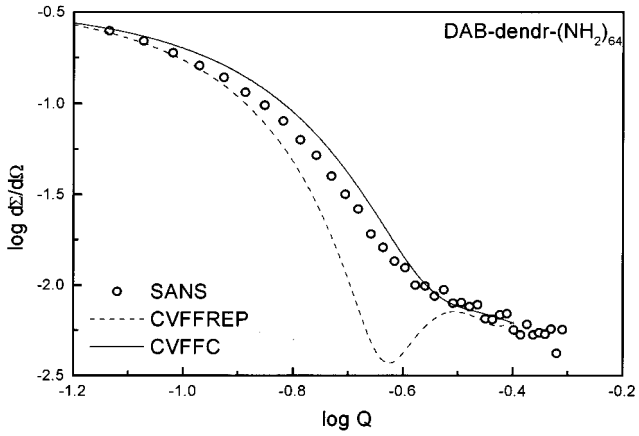

Figure 10. Double-logarithmic representation of the theoretical and experimental small-angle scattering curves of DAB-dendr-$(NH_2)_{64}$.

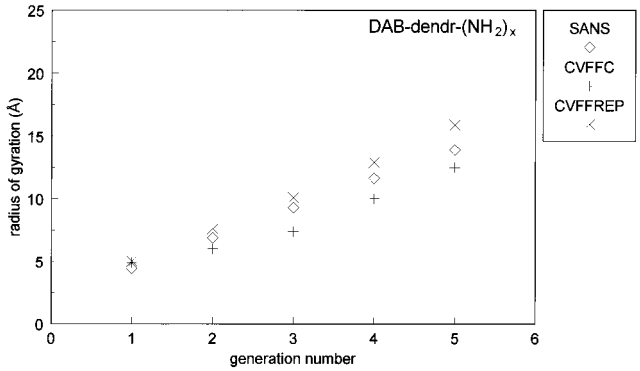

Figure 11. Comparison of the experimentally and theoretically determined radii of gyration for DAB-dendr-$(NH_2)_x$.

theoretical curves, does not show such clear features, indicating that the conformation of DAB-dendr-$(NH_2)_{64}$ in D_2O is less extended than the CVFFREP conformation (Figure 9b).

The average radii of gyration, calculated on the basis of the average conformations (Figure 9), and the experimentally determined radii of gyration (Table 1) are plotted in Figure 11. This figure nicely illustrates that the experimentally determined radii of gyration lie in between those calculated for the two extremes in solvent quality.

The experimental results and its comparison with the molecular dynamics calculations point to a compact structure, suggesting some degree of backfolding. This view is supported by the calculated probability distribution of the amine end groups in concentric shells, each of 1 Å thickness, from the core (Figure 12).

The probability distributions nicely illustrate that for both force fields the amine end groups are distributed throughout the dendrimer molecule. In the case of the CVFFREP force field there is an increasing probability going from the core to the periphery of the molecule while for the CVFFC force field there is a higher probability for the interior of the molecule, including the core region.

The corresponding average radial density distributions of DAB-dendr-$(NH_2)_x$ are depicted in Figure 13. These distributions give the density of segments in concentric shells, each of 1 Å thickness, about the center of mass. The calculated density of the first shells is highly inaccurate because they only contain a few atoms. For that reason, the first three shells have been

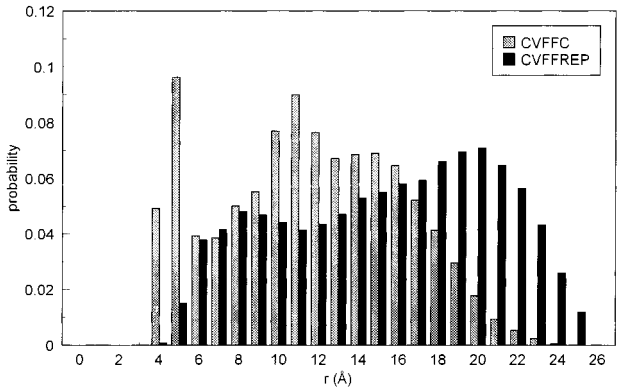

Figure 12. Probability distribution of the amine end groups in DAB-dendr-$(NH_2)_{64}$ for the two different force fields used (i.e., CVFFC and CVFFREP).

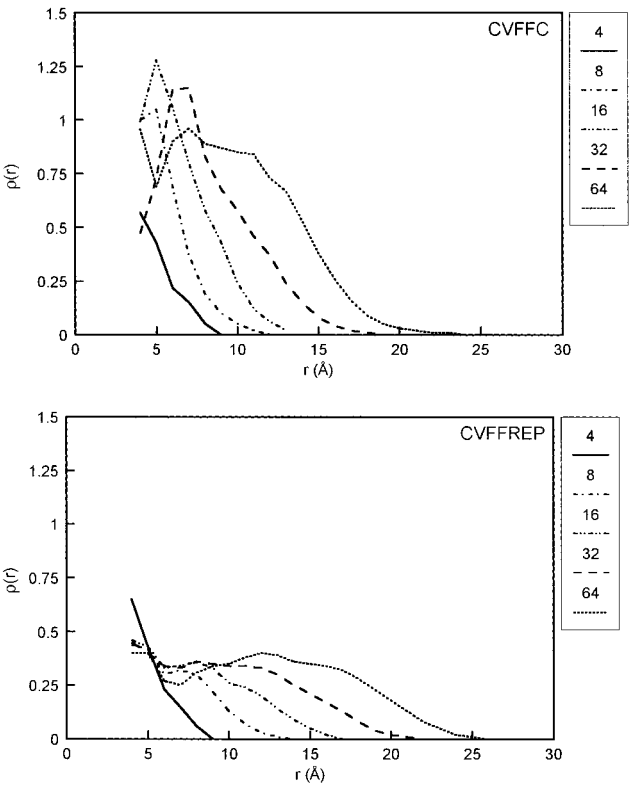

Figure 13. Average radial density distributions of DAB-dendr-$(NH_2)_x$ for the two different force fields used (i.e., CVFFC and CVFFREP).

omitted. The obtained radial density distributions are in good accordance with those described by Murat et al.[12] and Mansfield et al.[10] The density profiles exhibit a plateau region and a monotonic decrease of the density toward the exterior of the molecule. The length of the plateau region increases with increasing generation number and solvent quality, whereas the absolute density decreases with the solvent quality. The relatively homogeneous radial density distribution, especially at higher generations, is consistent with a compact (space-filling) structure.

4. Conclusions

The use of experimental techniques such as small-angle neutron scattering and viscosimetry in combination with molecular dynamics simulations proves to be quite efficient in achieving a better understanding of

the molecular characteristics of the poly(propyleneimine) dendrimers.

The dimension of these dendrimers increases linearly with the generation number and roughly as $M^{1/3}$ and is independent of the character of the end group and the solvent used. These results are indicative of a compact (space-filling) structure with a fractal dimensionality of approximately 3. The distinct maximum in the Kratky representation and the observed relation $R_\eta \simeq \sqrt{(5/3)}R_g$ are consistent with such a structure.

The molecular dynamics simulations on DAB-dendr-$(NH_2)_x$ reveal that the experimental scattering curve and radii of gyration lie in between those calculated for the different force fields. This is not unexpected because these force fields represent the limiting cases in solvent quality.

The above results suggest that DAB-dendr-$(NH_2)_{64}$ in D_2O is not an extended structure which indirectly implies some degree of backfolding in the poly(propyleneimine) dendrimers. This view is supported by the calculated probability distributions of the amine end groups. The corresponding radial density distributions display a constant density plateau and a monotonic decrease of the density toward the exterior of the molecule.

Summarizing, the experimental results and its comparison with the molecular dynamics calculations indicate that the poly(propyleneimine) dendrimers can be regarded as flexible molecules with a relatively homogeneous density distribution. Such an internal structure is not in line with the self-consistent-field model of de Gennes (i.e., dense shell)[8] or with the numerical simulations of Lescanec and Muthukumar[9] (i.e., dense core). It is precarious, however, to generalize these findings for other dendrimers because its internal structure is determined by a variety of parameters such as segment length, core and branch multiplicity as well as the chemical character and rigidity of the building blocks.

References and Notes

(1) Tomalia, D. A.; Baker, H.; Dewald, J.; Hall, M.; Kallos, G.; Martin, S.; Roeck, J.; Ryder, J.; Smith, P. *Polym. J.* **1985**, *17*, 117.
(2) Tomalia, D. A.; Naylor, A. M.; Goddard, W. A., III *Angew. Chem., Int. Ed. Engl.* **1990**, *29*, 138.
(3) Hawker, C. J.; Fréchet, J. M. J. *Macromolecules* **1990**, *23*, 4726.
(4) Morikawa, A.; Kamimoto, M.; Imai, Y. *Macromolecules* **1991**, *24*, 3469.
(5) Newkome, G. R.; Lin, X. *Macromolecules* **1991**, *24*, 1443.
(6) de Brabander-van den Berg, E. M. M.; Meijer, E. W. *Angew. Chem.* **1993**, *105*, 1370.
(7) Mourey, T. H.; Turner, S. R.; Rubinstein, M.; Fréchet, J. M. J.; Hawker, C. J.; Wooley, K. L. *Macromolecules* **1992**, *25*, 2401.
(8) de Gennes, P. G.; Hervet, H. J. *Phys. Lett. (Paris)* **1983**, *44*, 351.
(9) Lescanec, R. L.; Muthukumar, M. *Macromolecules* **1990**, *23*, 2280.
(10) Mansfield, M. L.; Klushin, L. I. *Macromolecules* **1993**, *26*, 4262.
(11) Mansfield, M. L. *Polymer* **1994**, *35*, 1827.
(12) Murat, M.; Grest, G. S. *Macromolecules* **1996**, *29*, 1278.
(13) Boris, D.; Rubinstein, M. *Macromolecules* **1996**, *29*, 7251.
(14) Meltzer, A. D.; Tirell, D. A.; Jones, A. A.; Inglefield, P. T.; Hedstrand, D. M.; Tomalia, D. A. *Macromolecules* **1992**, *25*, 4541.
(15) Meltzer, A. D.; Tirell, D. A.; Jones, A. A.; Inglefield, P. T. *Macromolecules* **1992**, *25*, 4549.
(16) Bauer, B. J.; Briber, R. M.; Hammouda, B.; Tomalia, D. A. *Polym. Mater. Sci. Eng.* **1992**, *67*, 428.
(17) Briber, R. M.; Bauer, B. J.; Hammouda, B.; Tomalia, D. A. *Polym. Mater. Sci. Eng.* **1992**, *67*, 430.
(18) Aharoni, S. M.; Murthy, N. S. *Polym. Commun.* **1983**, *24*, 132.
(19) de Brabander, E. M. M.; Brackman, J.; Mure-Mak, M.; de Man, H.; Hogeweg, M.; Keulen, J.; Scherrenberg, R.; Coussens, B.; Mengerink, Y.; van der Wal, S. *Macromol. Symp.* **1996**, *102*, 9.
(20) Scherrenberg, R. L.; Moonen, J., private communications.
(21) Guinier, A.; Forner, G. *Small-angle scattering of X-rays*; Wiley: New York, 1955.
(22) Di Pietro, G.; Joosten, J., private communications.
(23) Ramzi, A.; Scherrenberg, R.; Brackman, J.; Joosten, J.; Mortensen, K. *Macromolecules* **1997**, submitted for publication.
(24) Einstein, A. *Ann. Phys.* **1906**, *19*, 289.
(25) Computational results obtained using software programs from BIOSYM technologies of San Diego; molecular mechanics and dynamics calculations were performed with the *Discover* program, using the CVFF force field, and graphical displays were printed from the *Insight* II molecular moldeling system.
(26) van Vliet, P.; Edouard, G.; Coussens, B., private communications.
(27) Willner, L.; Jucknischke, O.; Richter, D.; Roovers, J.; Zhou, L.-L.; Roporowski, P. M.; Fetters, L. J.; Huang, J. S.; Lin, M. Y.; Hadjichristidis, N. *Macromolecules* **1994**, *27*, 3821.
(28) Grest, G. S.; Kremer, K.; Witten, T. A. *Macromolecules* **1987**, *20*, 1376.
(29) Antonietti, M.; Bremser, W.; Schmidt, M. *Macromolecules* **1990**, *23*, 3796.
(30) Roover, J.; Zhou, L.-L.; Toporowski, P. M.; van der Zwan, M.; Iatrou, H.; Hadjichristidis, N. *Macromolecules* **1993**, *26*, 4324.
(31) Sariban, A.; Brickman, J.; van Ruiten, J.; Meier, R. J. *Macromolecules* **1992**, *25*, 5950.

MA9618181